Comparative Evaluation of Molecular Representation Models for Simulation of Methane Adsorption on Graphtriyne Sheet

Noelia Faginas-Lago[1,2(✉)], Yusuf Bramastya Apriliyanto[3(✉)], Luca Mancini[1], and Andrea Lombardi[1,2]

[1] Dipartimento di Chimica, Biologia e Biotecnologie, Università degli Studi di Perugia, 06123 Perugia, Italy
noelia.faginaslago@unipg.it
[2] Istituto CNR di Scienze e Tecnologie Chimiche "Giulio Natta" (CNR-SCITEC), 06123 Perugia, Italy
[3] Department of Chemistry, Indonesia Defense University, Kampus Unhan Komplek IPSC Sentul, 16810 Bogor, Indonesia
yusuf.bramastya@gmail.com

Abstract. Reducing greenhouse gas emissions by employing advanced porous adsorbents is critical for mitigating anthropogenic contributions to the climate change. In this study, molecular dynamics (MD) simulations were performed to investigate the adsorption performance of graphtriyne sheet as a potential methane adsorbent. A comparative analysis of two molecular representation models—united-atom and atomistic—was conducted using the Improved Lennard-Jones (ILJ) potential function. The results indicated that the united-atom model yielded a higher permeation rate and diffusion coefficient but exhibited lower gas uptake than the atomistic model. The lack of orientation effects in the united-atom model led to reduced steric hindrance, facilitating methane permeation; whereas the atomistic model's stronger orientation effects lowered permeance. These findings highlight the significant influence of molecular representation on the accuracy of MD simulation results and emphasize the importance of selecting well-validated force field parameters for methane adsorption studies.

Keywords: MD simulations · graphynes · graphtriyne · methane capture

1 Introduction

Reducing greenhouse gases emissions is crucial in mitigating possible anthropic contributions to climate change and global warming. Methane (CH_4), a potent greenhouse gas, has been reported having a global warming potential (GWP) 84–87 times higher than carbon dioxide (CO_2) over a 20-year period and 28–36 times higher over a 100-year period [1,2]. Methane emissions contribute to about 30%

© The Author(s), under exclusive license to Springer Nature Switzerland AG 2026
O. Gervasi et al. (Eds.): ICCSA 2025 Workshops, LNCS 15897, pp. 17–27, 2026.
https://doi.org/10.1007/978-3-031-97660-5_2

of global warming, with annual emissions reaching approximately 570 million metric tons [3]. One effective strategy for reducing greenhouse gases emissions is the capture and storage of methane from anthropogenic sources such as landfills, coal mines, and natural gas processing facilities. Among various methane capture technologies, adsorption using advanced porous materials have actively been explored and garnered significant interest in the past few years due to its high efficiency, low energy consumption, and environmental sustainability [4–6].

Carbon-based materials bearing intrinsic pores currently have emerged as promising adsorbents for greenhouse gases due to their exceptional surface area, tunable porosity, and high chemical stability [7–9]. One notable form of carbon allotrope is graphene, a two-dimensional carbon-based nanomaterial. Unlike conventional porous adsorbents such as activated carbon, zeolites, and metal-organic frameworks (MOFs), graphene and its derivatives exhibit superior properties by having low density and robust structures originated from lightweight elements linked by strong covalent bonds [10]. Furthermore, functionalized graphene materials, including graphene oxide (GO) and reduced graphene oxide (rGO), have been studied for their enhanced adsorption properties, offering potential for large-scale methane capture and storage applications [11,12]. However, one significant limitation of graphene is its tendency to form aggregates, which restricts its gas uptake capacity. γ-graphynes are class of two-dimensional carbon allotropes that share several properties with graphene but offer the advantage of uniformly distributed and tunable pores [13]. Unlike graphene, γ-graphynes exhibit weaker dispersion forces, reducing aggregation. This characteristic makes them particularly effective for greenhouse gas capture [10,14]. Unfortunately, the effective way to experimentally synthesize graphines is not yet actively explored [15,16]. Within this gap, computational chemistry and molecular simulations have played a vital role in the development of carbon-based adsorbents for methane capture [17].

Density Functional Theory (DFT) calculations and Grand Canonical Monte Carlo (GCMC) simulations have been widely employed to predict methane adsorption behaviour, optimize pore structures, and enhance material performance [12,18]. These computational techniques provide valuable insights into the mechanisms of adsorption at the atomic level, facilitating the rational design of high-performance carbon-based adsorbents. Furthermore, molecular dynamics (MD) simulations have been increasingly utilized to investigate the dynamic interactions between methane molecules and graphene surfaces under different environmental conditions [19,20]. These simulations enable the analysis of key properties such as diffusion coefficients, adsorption energies, and interaction potentials, providing deeper insight into the stability and efficiency of graphene-based adsorbents for methane capture. MD simulations allow study of the adsorption kinetics, diffusion behavior, and structural stability of adsorbents over time, complementing the insights provided by the DFT and GCMC approaches [21]. Recent computational studies reported that graphtriyne (a form of graphynes, in which each benzene ring is connected to each of six others through a chain composed of three acetylenic bonds) [22] showed potential as a

carbon-based adsorbent for gas capture and separation under post-combustion conditions [23–26].

A critical aspect of computational simulations is the accurate representation of interatomic interactions as well as structural modeling of materials, which requires well-validated force field parameters [17,19]. The choice of force field influences the accuracy of adsorption predictions. Therefore, in this work, a comparative study of the two widely used molecular representations to model van der Waals interactions between methane and carbon-based materials is evaluated using extended MD simulations. The results could provide insights into the adsorption performance of graphtriyne for methane capture, by evaluating factors such as adsorption capacity and thermodynamic behaviour that contribute to the development of efficient methane adsorption technologies.

2 Theoretical Methods

For modelling the intermolecular interactions, the total potential energy of the system is split into electrostatic and non-electrostatic contributions. The electrostatic contribution is treated using a standard Coulombic summation, by assigning point charges of the interacting molecules as the following:

$$V_{tot}(r) = \sum_{i,j}^{n} \frac{q_i qj}{r_{ij}} + \sum_{i}^{n} V_{ILJ}(r_i) \tag{1}$$

On the other hand, the non-electrostatic term is expressed using the following Improved Lennard-Jones (ILJ) potential [27] which requires four parameters (r_0, ε, m and β) to be specified as given by

$$V_{ILJ}(r_i) = 4\varepsilon\left[\left(\frac{m}{m(r)-m}\right)\left(\frac{r_0}{r}\right)^{n(r)} - \frac{n(r)}{n(r)-m}\left(\frac{r_0}{r}\right)^{m}\right] \tag{2}$$

with

$$n(r) = \beta + 4.0\left(\frac{r}{r_0}\right)^2 \tag{3}$$

The r_0 and ε are pair specific parameter representing the equilibrium distance and the depth of potential well, respectively. The m parameter takes the value of 6 for describing interactions between neutral molecules. The β is an adjustable dimensionless parameter describing the hardness of the interaction. The ILJ formulation incorporates anisotropic effects and high-order interaction terms that refine the accuracy of intermolecular interactions, thus make ILJ as a versatile function that improve not only at equilibrium distance but also at short- and long-range parts of the potential compared to the Lennard-Jones (LJ) function [28].

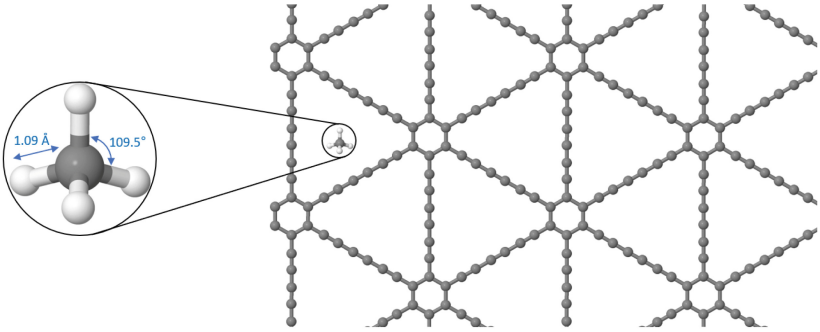

Fig. 1. Molecular geometry of methane and graphtriyne used in this study.

The methane molecular geometry has been optimized employing DFT at B3LYP/def2-TZVP level. The same computational strategy, based on DFT investigations, has been adopted in the past for several works [29–32], resulting as a valid compromise between chemical accuracy and computational cost. The graphtriyne structure is taken from Ref. [25] where it had been fully relaxed by using periodic DFT optimization. Figure 1 ilustrates the geometrical structure of methane and grapfhtriyne used in the MD simulations. Following computational approach reported in Ref. [20], a united-atom and an atomistic model were selected to represent methane molecule. The united-atom model treats the CH_4 molecule as a sphere by putting one interaction center on the center of mass of CH_4. On the other hand, the atomistic model puts an interaction center on all atoms of the CH_4 molecule. For the united-atom model, charges were calculated by the Hirshfeld population analysis [33] (–0.148 e on the carbon atom and 0.037 e on the hydrogen atoms). Meanwhile, for the atomistic model, the atomic charges of CH_4 molecule were not included meaning that all intermolecular interactions were operated by using only the ILJ potential. All parameters used for the simulations in this study (listed in Table 1) was taken from the parameters reported in Ref. [20].

Figure 2 shows the simulation box with dimension of $72.210 \times 62.523 \times 280.0$ $\mathring{A}^3$. A total of 100 CH_4 molecules were randomly distributed inside the simulation box, where graphtriyne sheet with a dimension of 72.210×62.523 $\mathring{A}^2$ was set in the center of the box. The cut-off distances for the ILJ and electrostatic interactions were set to 15 $\mathring{A}$, where the Ewald method [34] was applied for the calculation of electrostatic interactions. The graphtriyne were considered as a frozen framework and the gas molecules were treated as rigid bodies. Periodic boundary conditions were implemented in all directions of axes. Each simulation was performed for 5 ns after 0.5 ns equilibration period with a fixed time step of 1 fs. The statistical data and trajectory were collected at every 1 ps. All the MD simulations is performed by using DL_POLY package [35] in the canonical (NVT) ensemble employing the Nose-Hoover algorithm to maintain the applied

Table 1. Interaction parameters used for representing the intermolecular potentials in methane-graphtryne system. C_m indicates the C of the methane molecule.

Model	Type	ε (kcal mol^{-1})	$r_0(\AA)$	β	Charges (e)
United atom	Cm–Cm	0.421	4.168	8.215	–
	Cm–C	0.210	3.938	8.185	–
	Cm	–	–	–	–0.148
	H	–	–	–	0.037
Atomistic	Cm–Cm	0.109	3.800	8.027	–
	Cm–C	0.195	3.671	7.745	–
	Cm–H	0.075	3.628	4.932	–
	C–H	0.099	3.727	5.476	–
	H–H	0.005	3.419	4.363	–

temperatures at 300K. The graphical representations and the molecular trajectories were processed by using VMD program [36].

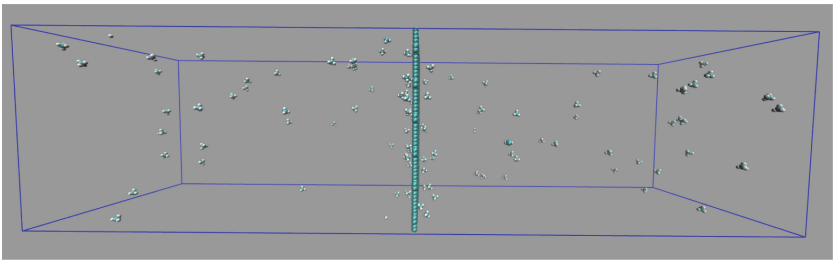

Fig. 2. Snapshoot of the simulation box filled with CH_4 molecules where the graphytriyne is located at the centre of simulation box.

3 Results and Discussion

Production runs of MD simulations were started after 0.5 ns equilibration time in which the energy and temperature convergence were checked as an indication of equilibrated system. Statistical data along with the z-density and the radial distribution function (RDF) profiles were then monitored. Figure 3 depicts the fluctuation of configurational energy during the simulation period. We obtained the average configuration energy or potential energy for the united atom model of –45.59 kcal mol^{-1} with a percent deviation of about 12% or equal to 5.63 kcal mol^{-1}. On the other hand, the average value for the atomistic model is about –360.60 kcal mol^{-1} with 7% deviation or equal to 25.28 kcal mol^{-1}. This confirmed that classical MD simulations of diverse models exhibited different energy

fluctuations; in this case, the united atom model had more potential energy fluctuation at the equilibrium. Interestingly, the atomistic model produced more converge and more negative potential energy surface at the equilibrium that could be an early indication of high adsorption phenomenon.

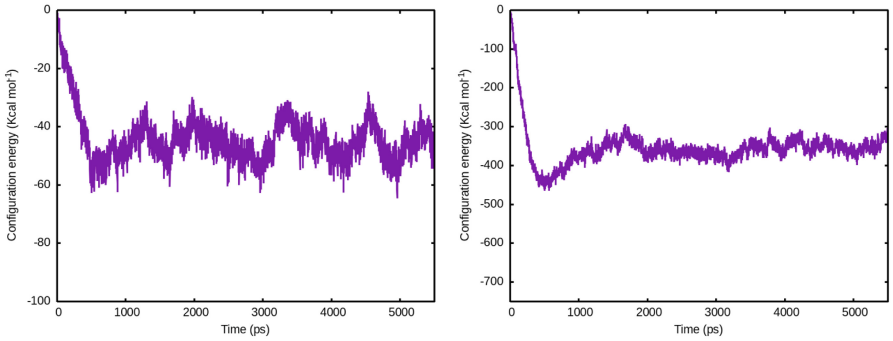

Fig. 3. Configurational energy fluctuation of united atom (left panel) and atomistic model (right panel) during MD simulations.

The CH_4 molecules could cross the layer multiple times from both sides of the layer during the production runs (see the snapshoot reported in Fig. 2). The number of permeation events was then calculated and plotted as a function of simulation time. The slope of this plot is an estimation of the CH_4 permeation rate measured in a unit of molecules ps^{-1}. Figure 4 (left panel) depicts the permeation events as a function of time for the united-atom and atomistic model of CH_4. It is clear that the number of permeation events of CH_4 represented by using united-atom model is higher than the atomistic model. Quantitatively, permeation rate of CO_2 for the united-atom model is 1.419×10^{-1} molecules ps^{-1}, almost 60% higher than its counterpart by only 0.905×10^{-1} molecules ps^{-1}.

Figure 4 (right panel) shows a plot of the mean number density of CH_4 along the z-axis (i.e. the z-density profile), where the z-axis is perpendicular with the graphtriyne surface. As it can be seen from the z-density profile, there are sharp peaks at a region below 5 $\mathring{A}$ from the surface. This region is the location where CH_4 molecules are highly adsorbed by the graphtriyne, thus it is normally called as the adsorption region. Surprisingly, a high permeation rate of CH_4 for the united-atom model is inversely related to the CH_4 adsorption on the graphtriyne surface (Fig. 4, right panel). As reported in our previous works [23–25], the permeation events are closely related to the adsorption of gas over the surfaces of membrane. The more gas is adsorbed over the surfaces, the higher is its probability to permeate the graphtriyne sheet. However, the number of adsorbed molecules also can diminish the gas permeance by saturating the pores and blocking other molecules to cross the membrane. Apparently, this

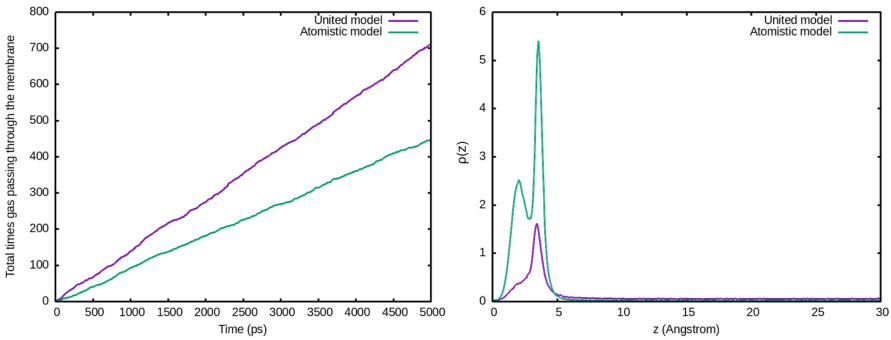

Fig. 4. Permeation events as a function of time (left panel) and the z-density profiles (right panel) for CH_4 represented as united-atom and atomistic model.

phenomenon happened for the case of CH_4 treated using atomistic model, where the atomistic model produced stronger attraction forces combined with orientation requirement for crossing the graphtriyne leading to lower gas permeance than the united-atom model.

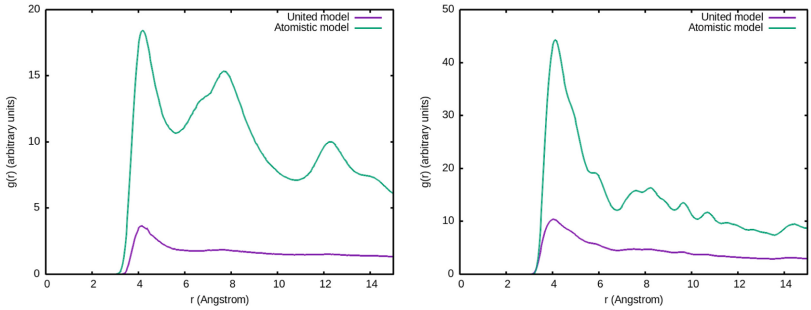

Fig. 5. Radial distribution functions (RDF) between CH_4 molecules (right) and CH_4 molecules with respect to graphtryne (left) for united-atom and atomistic model.

Stronger attraction forces for the case of atomistic model can also be verified by looking at the radial distribution functions (RDF) reported in Fig. 5. According to RDF, atomistic model has the largest and highest peaks meaning that CH_4 molecules are more likely to be located near the C atoms of graphtriyne and near other CH_4 molecules. In other words, high and broad peaks of RDF presented in Fig. 5 correspond to the deep and wide of CH_4 potential well, meaning a strong long-ranged attractions, when CH_4 is represented by using atomistic model. In addition to the RDF reported in Fig. 5, the stronger attraction for atomistic model is also reflected in configuration and vdW energies listed in Table 2. The

atomistic model produced more negative energies, even two orders of magnitude lower than the united-atom model. Table 2 also shows that for the case of united model, the contribution of Coulombic energy is quite small; this indicates the electrostatic interactions between non-polar molecules are weak and negligible in comparison with the van der Waals forces. Therefore, the adsorption dynamics of CH_4 molecules on grapthriyne sheet is mainly governed by van der Waals intermolecular interactions.

Table 2. Several key properties of methane adsorption on graphtriyne obtained from the MD simulations

Parameters	United Model	Atomistic model
Configuration Energy (kcal mol^{-1})	-4.559×10^{1}	-3.606×10^{2}
vdW Energy (kcal mol^{-1})	-4.559×10^{1}	-3.606×10^{2}
Couloumb Energy (kcal mol^{-1})	-1.493×10^{-4}	–
Diffusion Coefficient (10^{-9} m^2s^{-1})	3.211×10^{3}	1.415×10^{3}
Adsorbed Molecules (molecules)	24.669	80.621
Gas Permeation Rate (molecules ps^{-1})	1.419×10^{-1}	0.905×10^{-1}

We also calculated the average of CH_4 uptakes by integrating the z-density profiles at the adsorption region. The adsorption region is an area located in the range of 5 $\mathring{A}$ from the surface of graphtriyne. We found that the atomistic model yielded a much stronger methane adsorption by capturing about 81 molecules. The united-atom model, on the other hand, showed a lower methane uptake of 25 molecules (Table 2). This trend is in good agreement with the results reported in Ref. [20], where the atomistic model of methane predicted more CH_4 adsorption on graphene surface. Furthermore, by calculating the diffusion coefficient of methane (defined as the rate of CH_4 movement inside the simulation box), we confirm that the atomistic model exhibits stronger adsorption by the fact that attraction forces could impede the movement of CH_4 molecules, decreasing the diffusion coefficient value (Table 2). As a final remark, both molecular representation models reveal the potential application of graphtriyne for methane adsorption. However, it is clear that the choice of force field influences the accuracy of adsorption predictions; therefore, it is crucial to use the appropriate set of force fields to guarantees a quantitative description of the interactions and trustable results for the adsorption dynamics.

4 Conclusions

Graphtriyne sheet has been investigated for the purpose of methane capture employing extensive MD simulations based on two distinct formulation of force fields. The results showed that graphtriyne sheet could be considered as a potential porous adsorbent for methane gas uptake. Comparative analysis of

two molecular representation models of CH_4 (i.e. united-atom and atomistic) revealed that the united-atom model produced higher permeation rate and diffusion coefficient than the later. Conversely, the united-atom model exhibited lower gas uptake than the atomistic model. The united-atom model did not take into account orientation effects for the representation of CH_4 molecules. Therefore, within this model, adsorbed molecules around the pores did not spent time too long for crossing the graphtriyne sheet; in other words, there was no steric hindrance that preventing permeation events. However, the orientation effects were found stronger for the atomistic gas model, lowering the CH_4 permeance. In addition, we found that the adsorption dynamics of CH_4 molecules on grapthriyne sheet was mainly governed by van der Waals forces. The type of molecular representation highly influences the accuracy of MD simulations results, yet more details representation requires more computational time. Considering all those results, the choice of well-validated force field parameters is a critical aspect of molecular simulations. Improving future force fields should focus on incorporating molecular orientation effects and steric barriers into simplified models to enhance the accuracy of adsorption and diffusion studies, while still optimizing computational efficiency.

Acknowledgments. This work has been funded by the European Union - NextGenerationEU under the Italian Ministry of University and Research (MUR) National Innovation Ecosystem grant ECS00000041 - VITALITY - CUP J97G22000170005. N.F.L thanks financial support under the National Recovery and Resilience Plan (NRRP), Mission 4, Component 2, Investment 1.1, Call for tender No. 104 published on 2.2.2022 by the Italian Ministry of University and Research (MUR), funded by the European Union – NextGenerationEU – Project Title 2022JC2Y93 ChemicalOrigins: linking the fossil composition of the Solar System with the chemistry of protoplanetary disks – CUP J53D23001600006 - Grant Assignment Decree No. 962 adopted on 30/06/2023 by the Italian Ministry of University and Research (MUR). A.L. acknowledges funding by the Italian Ministry of Environment and Energy Security in the framework of the Project GoPV (CSEAA_00011) for Research on the Electric System. YBA acknowledges support from the Department of Chemistry Unhan RI

Disclosure of Interests. The authors have no competing interests to declare that are relevant to the content of this article.

References

1. WRI: How methane emissions contribute to climate change. https://www.wri.org/. Accessed 01 Mar 2025
2. UNEP: Global methane assessment: Benefits and costs of mitigating methane emissions. unep & climate and clean air coalition. https://www.unep.org/resources. Accessed 01 Mar 2025
3. IEA: Methane tracker 2021: Methane and climate change. https://www.iea.org/reports/methane-tracker-2021. Accessed 01 Mar 2025
4. Alonso, A., et al.: Critical review of existing nanomaterial adsorbents to capture carbon dioxide and methane. Sci. Total Environ. **595**, 51–62 (2017).

https://doi.org/10.1016/j.scitotenv.2017.03.229. https://www.sciencedirect.com/science/article/pii/S004896971730760X
5. Roohollahi, H., Zeinalzadeh, H., Kazemian, H.: Recent advances in adsorption and separation of methane and carbon dioxide greenhouse gases using metalâorganic framework-based composites. Ind. Eng. Chem. Res. **61**(30), 10555–10586 (2022). https://doi.org/10.1021/acs.iecr.2c00664
6. Ko, V.Y., Wang, J., He, I., Ryan, D., Zhang, X., Lan, C.: Adsorption of methane on biochar for emission reduction in oil and gas fields. Biochar **5**(1), 15 (2023)
7. Memetova, A., et al.: Porous carbon-based material as a sustainable alternative for the storage of natural gas (methane) and biogas (biomethane): a review. Chem. Eng. J. **446**, 137373 (2022). https://doi.org/10.1016/j.cej.2022.137373. https://www.sciencedirect.com/science/article/pii/S1385894722028613
8. Singh, R., Wang, L., Ostrikov, K.K., Huang, J.: Designing carbon-based porous materials for carbon dioxide capture. Adv. Mater. Interfaces **11**(4), 2202290 (2024). https://doi.org/10.1002/admi.202202290. https://advanced.onlinelibrary.wiley.com/doi/abs/10.1002/admi.202202290
9. Deng, H., Li, T., Li, H., Dang, A., Han, Y.: Carbon-based adsorbents for co2 capture: a systematic review. J. Ind. Eng. Chem. (2024). https://doi.org/10.1016/j.jiec.2024.12.026. https://www.sciencedirect.com/science/article/pii/S1226086X24008396
10. de Oliveira, R.B., Borges, D.D., Machado, L.D.: Mechanical and gas adsorption properties of graphene and graphynes under biaxial strain. Sci. Rep. **12**(1), 22393 (2022). https://doi.org/10.1038/s41598-022-27069-y
11. Szczniak, B., Choma, J., Jaroniec, M.: Gas adsorption properties of graphene-based materials. Adv. Colloid Interface Sci. **243**, 46–59 (2017). https://doi.org/10.1016/j.cis.2017.03.007. https://www.sciencedirect.com/science/article/pii/S0001868617300039
12. Arango Hoyos, B.E., et al.: Exploring the capture and desorption of co2 on graphene oxide foams supported by computational calculations. Sci. Rep. **13**(1), 14476 (2023). https://doi.org/10.1038/s41598-023-41683-4
13. James, A., et al.: Graphynes: indispensable nanoporous architectures in carbon flatland. RSC Adv. **8**, 22998–23018 (2018). https://doi.org/10.1039/C8RA03715A
14. Azizi, K., Vaez Allaei, S.M., Fathizadeh, A., Sadeghi, A., Sahimi, M.: Graphyne-3: a highly efficient candidate for separation of small gas molecules from gaseous mixtures. Sci. Rep. **11**(1), 16325 (2021). https://doi.org/10.1038/s41598-021-95304-z
15. Desyatkin VG, Martin WB, A.A.: Scalable synthesis and characterization of multilayer -graphyne, new carbon crystals with a small direct band gap. J. Am. Chem. Soc. **144**(39), 17999–18008 (2022). https://doi.org/10.1021/jacs.2c06583
16. Li, J., Han, Y.: Artificial carbon allotrope γ-graphyne: synthesis, properties, and applications. Giant **13**, 100140 (2023)
17. Vekeman, J., Cuesta, I. G., Faginas-Lago, N., Wilson, J., Snchez-Marn, J., Snchez de Mers, A.: Potential models for the simulation of methane adsorption on graphene: development and ccsd(t) benchmarks. Phys. Chem. Chem. Phys. **20**, 25518–25530 (2018). https://doi.org/10.1039/C8CP03652G
18. Rugarabamu, J.R., Zhao, D., Li, S., Diao, R., Song, K.: Structure modeling of activated carbons used for simulating methane adsorption- a review. Petrol. Res. **8**(1), 103–117 (2023)
19. Vekeman, J., Sanchez-Marin, J., Sanchez de Meras, A., Garcia Cuesta, I., Faginas-Lago, N.: Flexibility in the graphene sheet: the influence on gas adsorption from molecular dynamics studies. J. Phys. Chem. C **123**(46), 28035–28047 (2019)

20. Vekeman, J., Faginas-Lago, N., Lombardi, A., Sánchez de Merás, A., García Cuesta, I., Rosi, M.: Molecular dynamics of ch_4/n_2 mixtures on a flexible graphene layer: adsorption and selectivity case study. Front. Chem. **7**, 386 (2019)
21. Faginas-Lago, N., Apriliyanto, Y.B., Lombardi, A.: Confinement of co_2 inside carbon nanotubes. Eur. Phys. J. D **75**(5), 161 (2021)
22. Bartolomei, M., Carmona-Novillo, E., Giorgi, G.: First principles investigation of hydrogen physical adsorption on graphynes' layers. Carbon **95**, 1076–1081 (2015)
23. Faginas-Lago, N., Apriliyanto, Y.B., Lombardi, A.: Molecular simulations of $co_2/n_2/h_2o$ gaseous mixture separation in graphtriyne membrane. In: Misra, S., et al. (eds) ICCSA 2019. Lecture Notes in Computer Science, pp. 374–387. Springer, Heidelberg (2019)
24. Faginas-Lago, N., Apriliyanto, Y.B., Lombardi, A.: Carbon capture and separation from co2/n2/h2o gaseous mixtures in bilayer graphtriyne: a molecular dynamics study. In: Gervasi, O., et al. (eds.) ICCSA 2020. LNCS, vol. 12255, pp. 489–501. Springer, Cham (2020). https://doi.org/10.1007/978-3-030-58820-5_36
25. Apriliyanto, Y.B., et al.: Multilayer graphtriyne membranes for separation and storage of co2: Molecular dynamics simulations of post-combustion model mixtures. Molecules **27**(18), 5958 (2022)
26. Bartolomei, M., Giorgi, G.: A novel nanoporous graphite based on graphynes: first-principles structure and carbon dioxide preferential physisorption. ACS Appl. Mater. Interfaces **8**, 27996–28003 (2016). https://doi.org/10.1021/acsami.6b08743
27. Pirani, F., Brizi, S., Roncaratti, L.F., Casavecchia, P., Cappelletti, D., Vecchiocattivi, F.: Beyond the lennard-jones model: a simple and accurate potential function probed by high resolution scattering data useful for molecular dynamics simulations. Phys. Chem. Chem. Phys. **10**(36), 5489–5503 (2008)
28. Bramastya Apriliyanto, Y., Lombardi, A., Mancini, L., Pirani, F., Faginas-Lago, N.: Revisiting numerical solutions of weakly bound noble gases' vibrational energy levels modeled by the improved lennard-jones potential. ChemPhysChem **25**(20), e202400223 (2024)
29. Pannacci, G., et al.: A combined crossed molecular beam and theorerical study of the o (3 p, 1 d)+ acrylonitrile (ch 2 chcn) reactions and implications for combustion and extraterrestrial environments. Phys. Chem. Chem. Phys. **25**(30), 20194–20211 (2023)
30. Liang, P., et al.: Oh (2π)+ c2h4 reaction: a combined crossed molecular beam and theoretical study. J. Phys. Chem. A **127**(21), 4609–4623 (2023)
31. Giani, L., et al.: Revised gas-phase formation network of methyl cyanide: the origin of methyl cyanide and methanol abundance correlation in hot corinos. Mon. Not. R. Astron. Soc. **526**(3), 4535–4556 (2023)
32. Richardson, V., et al.: Fragmentation of interstellar methanol by collisions with he+: an experimental and computational study. Phys. Chem. Chem. Phys. **24**(37), 22437–22452 (2022)
33. Hirshfeld, F.: Bonded-atom fragments for describing molecular charge densities. Theor. Chim. Acta **44**, 129–138 (1977). https://doi.org/10.1007/BF00549096
34. Ewald, P.P.: Die berechnung optischer und elektrostatischer gitterpotentiale. Annalen der Physik **369**(3), 253–287 (1921). https://doi.org/10.1002/andp.19213690304. https://onlinelibrary.wiley.com/doi/abs/10.1002/andp.19213690304
35. Smith, W., Yong, C.W., Rodger, P.M.: Dl_poly: application to molecular simulation. Molec. Simul. **28**, 385 – 471 (2002). https://api.semanticscholar.org/CorpusID:95419206
36. Humphrey, W., Dalke, A., S.K.: VMD: visual molecular dynamics. J. Mol. Graph. **14**, 33–28 (1996). https://doi.org/10.1016/0263-7855(96)00018-5